Letters

Digital Implementation of an Adaptive Speed Regulator for a PMSM

Han Ho Choi, Nga Thi-Thuy Vu, and Jin-Woo Jung

***Abstract*—We design an adaptive speed regulator for a permanent-magnet synchronous motor (PMSM). The proposed adaptive regulator does not require any information on the PMSM parameter and load-torque values, thus, it is insensitive to model parameter and load-torque variations. We implement the proposed adaptive-speed-regulator system by using a TMS320F28335 floating point DSP. We give simulation and experimental results to verify that our method can be successfully used to control a PMSM under model parameter and load-torque variations.**

***Index Terms*—Adaptive-control system, disturbance, permanent-magnet synchronous motor (PMSM), uncertainty.**

I. Introduction

A PERMANENT-MAGNET synchronous motor (PMSM) has been widely employed in servo applications such as chip-mount machines, robotics, and hard disk drives because it features low noise, low inertia, high efficiency, and low maintenance cost. However, a PMSM cannot be easily controlled because of the uncertainties such as parameter variations and load-torque variations. Therefore, the linear-control methods such as PID control cannot guarantee high performance. To solve this problem, many researchers have proposed various design methods, e.g., adaptive control [1]–[4], nonlinear feedback linearization control [5], and fuzzy control [6], [7]. Recently, several authors [8]–[10] have proposed disturbance-observer-based PMSM control methods that can effectively suppress load-torque variations. However, most of the previous PMSM control design methods cannot guarantee stability and convergence of speed error responses under inexact information on the PMSM parameters such as the stator resistance, the stator inductance, the rotor inertia, the viscous friction coefficient, the magnetic flux, etc. Considering these facts, we propose an adaptive-control law design method for a PMSM. We first design an adaptive speed regulator which does not require any information on the PMSM parameter and load-torque values. We also prove that the speed error of the closed-loop system converges to zero and the parameter adaptation error signal is bounded. Finally, simulation and experimental results are shown to verify that the proposed method can precisely control the speed of a PMSM under model parameter and load-torque variations.

Manuscript received March 17, 2010; revised May 25, 2010; accepted June 23, 2010. Date of current version December 27, 2010. This work was supported by Basic Science Research Program through the National Research Foundation (NRF) of Korea funded by the Ministry of Education, Science, and Technology (2010-0015428) and by the Dongguk Research Fund. Recommended for publication by Associate Editor R. Burgos.

The authors are with the Division of Electronics and Electrical Engineering, Dongguk University - Seoul, Seoul 100-715, Korea (e-mail: jinwjung@dongguk.edu).

Color versions of one or more of the figures in this paper are available online at http://ieeexplore.ieee.org.

Digital Object Identifier 10.1109/TPEL.2010.2055890

II. Model Description

By taking the rotor coordinates of the motor as reference coordinates, a surface-mounted PMSM can be represented by the following nonlinear equation:

$$\begin{cases} \dot{\omega} = k_1 i_{qs} - k_2 \omega - k_3 T_L \\ \dot{i}_{qs} = -k_4 i_{qs} - k_5 \omega - \omega i_{ds} + k_6 V_{qs} + d_q \\ \dot{i}_{ds} = -k_4 i_{ds} + \omega i_{qs} + k_6 V_{ds} + d_d \end{cases} \tag{1}$$

where T_L represents the load torque, ω is the electrical rotor angular speed, i_{qs} is the q-axis current, V_{qs} is the q-axis voltage, i_{ds} is the d-axis current, V_{ds} is the d-axis voltage, d_q and d_d represent disturbance inputs, and $k_i > 0, i = 1, \ldots, 6$ are the parameter values depending on the number of poles, the stator resistance, the stator inductance, the rotor inertia, the viscous friction coefficient, and the magnetic flux. The load-torque disturbance term T_L and uncertainties on the parameters k_i can severely deteriorate the control performance if they are not appropriately accounted for.

We will use the following assumptions:

A1: ω, i_{qs}, and i_{ds} are available.

A2: The desired speed ω_d is constant and $\dot{\omega}_d = \ddot{\omega}_d = 0$.

A3: T_L is unknown, $\dot{T}_L$ can be set as $\dot{T}_L = 0$.

A4: k_i are not known accurately, $\dot{k}_i$ can be set as $\dot{k}_i = 0$.

A5: d_q and d_d are unknown, $\dot{d}_q$ and $\dot{d}_d$ can be set as $\dot{d}_q = \dot{d}_d = 0$.

We will denote the electrical rotor angular acceleration $\dot{\omega}$ by $\beta = k_1 i_{qs} - k_2 \omega - k_3 T_L = \dot{\omega}$. Then, by introducing the speed error $\omega_e = \omega - \omega_d$ and by denoting V_{qf} and V_{df} as

$$\begin{cases} V_{qf} = \dfrac{1}{k_6}(k_4 i_{qs} + k_5 \omega + \omega i_{ds} - d_q) \\ \qquad\quad + \dfrac{1}{k_1 k_6}[k_2 - \gamma_q]\beta \\ V_{df} = \dfrac{1}{k_6}(k_4 i_{ds} - \omega i_{qs} - d_d) \end{cases} \tag{2}$$

we can obtain the following error dynamics

$$\begin{cases} \dot{\omega}_e = \beta \\ \dot{\beta} = -\gamma_q \beta + k_1 k_6 (V_{qs} - V_{qf}) \\ \dot{i}_{ds} = k_6 (V_{ds} - V_{df}) \end{cases} \tag{3}$$

where $\gamma_q > 0$ is a constant design parameter.

After all, our design problem can be formulated as designing an adaptive control law $[V_{qs}, V_{ds}]^T$ for the aforementioned error dynamics (3).

Before proceeding further, we give a background result which will be used to derive our main results.

Lemma 1: There exist constant parameter vectors $\xi_q^* = [\xi_{q1}^*, \xi_{q2}^*, \xi_{q3}^*, \xi_{q4}^*]^T$ and $\xi_d^* = [\xi_{d1}^*, \xi_{d2}^*, \xi_{d3}^*]^T$ such that

$$h_q^T \xi_q^* = \sum_{i=1}^{4} h_{qi}\xi_{qi}^* = V_{qf}, h_d^T \xi_d^* = \sum_{i=1}^{3} h_{di}\xi_{di}^* = V_{df} \quad (4)$$

where $h_q = [h_{q1}, h_{q2}, h_{q3}, h_{q4}]^T = [\omega, i_{qs}, \omega i_{ds}, 1]^T$ and $h_d = [h_{d1}, h_{d2}, h_{d3}]^T = [i_{ds}, \omega i_{qs}, 1]^T$.

Proof: The assumptions A3–5 imply that (4) holds with $\xi_d^* = [k_4, -1, -d_d]^T / k_6$ and

$$\xi_q^* = \frac{1}{k_1 k_6}\begin{bmatrix} (k_2\gamma_q - k_2^2 + k_1 k_5) \\ k_1(k_2 - \gamma_q + k_4) \\ k_1 \\ (\gamma_q k_3 T_L - k_2 k_3 T_L - k_1 d_q) \end{bmatrix}. \quad (5)$$

▽ ▽ ▽

III. Adaptive Controller Design and Stability Analysis

Theorem 1: Let the control input variables V_{qs} and V_{ds} be given by the following adaptive control law:

$$V_{qs} = -\delta_q\sigma_q + \sum_{i=1}^{4}\xi_{qi}h_{qi}, V_{ds} = -\delta_d i_{ds} + \sum_{i=1}^{3}\xi_{di}h_{di} \quad (6)$$

$$\xi_{qi} = -\frac{1}{\phi_{qi}}\int_0^t h_{qi}\sigma_q d\tau, \xi_{di} = -\frac{1}{\phi_{di}}\int_0^t h_{di} i_{ds} d\tau \quad (7)$$

where ξ_{qi} and ξ_{di} are estimates of ξ_{qi}^* and ξ_{di}^*, $\sigma_q = \gamma_q\omega_e + \beta$, $\phi_{qi} > 0$, $\phi_{di} > 0$, $\delta_q > 0$, and $\delta_d > 0$. Then, ω_e converges to zero, ξ_{qi} and ξ_{di} are bounded.

Proof: Along the similar line of [12], we will show the stability of the adaptive system. Let us define the Lyapunov functional as $V(t) = \sigma_q^2 + i_{ds}^2 + \sum_{i=1}^4 k_1 k_6 \phi_{qi}\tilde{\xi}_{qi}^2 + \sum_{i=1}^3 k_6\phi_{di}\tilde{\xi}_{di}^2$, where $\tilde{\xi_{qi}} = \xi_{qi}^* - \xi_{qi}$ and $\tilde{\xi_{di}} = \xi_{di}^* - \xi_{di}$. Its time derivative along the error dynamics (3) is given by

$$2\dot{V} = \sigma_q\dot{\sigma}_q + i_{ds}\dot{i}_{ds} - \sum_{i=1}^{4} k_1 k_6\phi_{qi}\tilde{\xi_{qi}}\dot{\xi}_{qi} - \sum_{i=1}^{3} k_6\phi_{di}\tilde{\xi_{di}}\dot{\xi}_{di}. \quad (8)$$

On the other hand, (3) implies that

$$\dot{\sigma}_q = -k_1 k_6(V_{qf} - V_{qs}), \dot{i}_{ds} = -k_6(V_{df} - V_{ds}). \quad (9)$$

Lemma 1, (6), and (7) imply that

$$\begin{cases} V_{qs} = -\delta_q\sigma_q + V_{qf} - \sum_{i=1}^{4}\tilde{\xi}_{qi}h_{qi} \\ V_{ds} = -\delta_d i_{ds} + V_{df} - \sum_{i=1}^{3}\tilde{\xi}_{di}h_{di} \end{cases} \quad (10)$$

$$\dot{\xi}_{qi} = -\frac{1}{\phi_{qi}}h_{qi}\sigma_q, \dot{\xi}_{di} = -\frac{1}{\phi_{di}}h_{di}i_{ds} \quad (11)$$

therefore, (8) can be reduced to

$$2\dot{V} \le -k_1 k_6\delta_q\sigma_q^2 - \delta_d k_6 i_{ds}^2 \le 0 \quad (12)$$

where $k_i > 0$, $\delta_q > 0$, and $\delta_d > 0$ are used. The inequality (12) implies that

$$2\int_0^\infty \dot{V}(\tau)d\tau \le -k_1 k_6\delta_q\int_0^\infty \sigma_q^2 d\tau - \delta_d k_6\int_0^\infty i_{ds}^2 d\tau. \quad (13)$$

Multiplying (13) by -1 and integrating the left-hand side of (13) give

$$k_1 k_6\delta_q\int_0^\infty \sigma_q^2 d\tau + \delta_d k_6\int_0^\infty i_{ds}^2 d\tau \le 2V(0) \quad (14)$$

where $V(t) \ge 0$ is used. Because $k_1 k_6\delta_q > 0$ and $\delta_d k_6 > 0$, we can obtain

$$\int_0^\infty \sigma_q^2 d\tau < \infty \quad (15)$$

which implies that $\sigma_q \in L_2$. Since $\dot{V} \le 0$ as shown in (12), we can see that $V(t)$ is nonincreasing and is upper bounded as $V(t) \le V(0)$. This implies that $\sigma_q \in L_\infty$, $i_{ds} \in L_\infty$, $\xi_q \in L_\infty$, and $\xi_d \in L_\infty$. Because of the transfer function from σ_q to ω_e, $H_{\omega_e\sigma_q}(s)$ is strictly positive real, and $\sigma_q \in L_2$, we can use the result of [12] to state that ω_e converges to zero.

▽ ▽ ▽

IV. Discretized Controller

We can rearrange V_{qs} and V_{ds} as

$$V_{qs} = u_{qs} + u_{qd}, V_{ds} = u_{ds} + u_{dd}, \quad (16)$$

where u_{qs} and u_{ds} are the static terms given by

$$u_{qs}(t) = -\delta_q\gamma_q\omega_e, u_{ds}(t) = -\delta_d i_{ds} \quad (17)$$

and $u_{qd}(t)$ and $u_{dd}(t)$ are the dynamic terms given by

$$u_{qd}(t) = -\delta_q\frac{d}{dt}\omega_e - \sum_{i=1}^{4} h_{qi}\xi_{qi}, u_{dd}(t) = -\sum_{i=1}^{3}\xi_{di}h_{di}. \quad (18)$$

For digital implementation under a sufficiently small sampling time T, the static terms u_{qs} and u_{ds} at the sampling instant kT can be straightforwardly set as

$$u_{qs}(k) = -\delta_q\gamma_q\omega_e(k), u_{ds}(k) = -\delta_d i_{ds}(k) \quad (19)$$

whereas the dynamic terms $u_{qd}(k)$ and $u_{dd}(k)$ cannot be straightforwardly obtained. By using the relation $\dot{\omega} = \beta$ and the previous result [11], we can compute the derivative term $\beta(k)$ by using the following recursive equation:

$$\beta(k) = \frac{\rho}{T + \rho}\beta(k-1) + \frac{1}{T + \rho}[\omega(k) - \omega(k-1)] \quad (20)$$

where ρ is a sufficiently small filter time constant to limit the susceptibility of the derivative term $\beta = \dot{\omega}$ to noise. By using the relation (7) and the previous result [11], we can compute the integral terms $\xi_{qi}(k)$ and $\xi_{di}(k)$ by using the following recursive

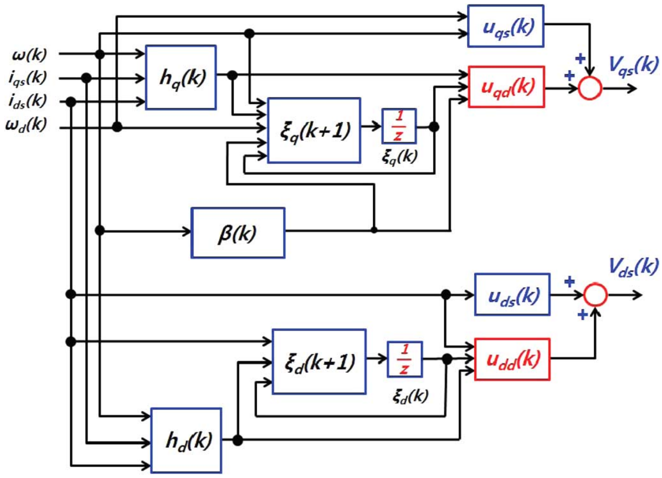

Fig. 1. Block diagram of the proposed control algorithm.

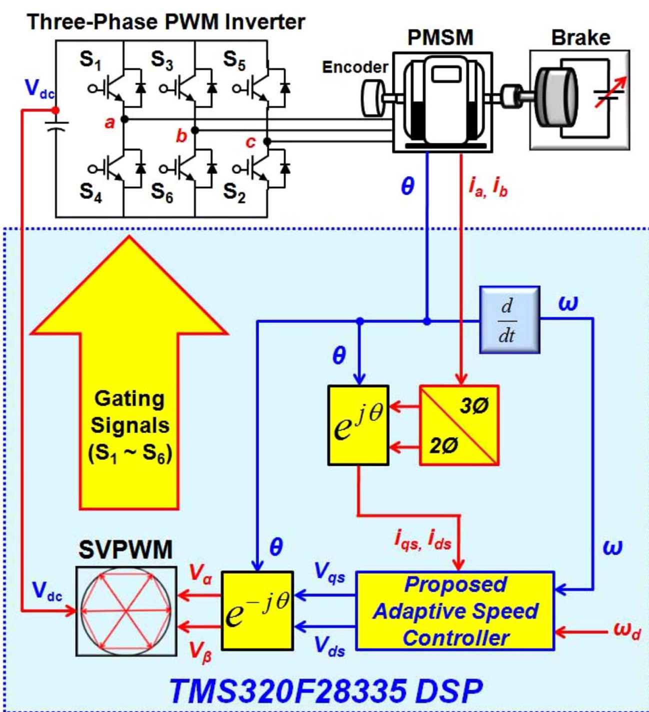

Fig. 2. Block diagram of the proposed PMSM control system.

equation:

$$\xi_{qi}(k+1) = \xi_{qi}(k) - \frac{T}{\phi_{qi}} h_{qi}(k)[\gamma_q \omega_e(k) + \beta(k)] \quad (21)$$

$$\xi_{di}(k+1) = \xi_{di}(k) - \frac{T}{\phi_{di}} h_{di}(k) i_{ds}(k). \quad (22)$$

And, therefore, the dynamic terms $u_{qd}(k)$ and $u_{dd}(k)$ can be computed by the following equation:

$$\begin{cases} u_{qd}(k) = -\delta_q \beta(k) + \sum_{i=1}^{4} \xi_{qi}(k) h_{qi}(k) \\ u_{dd}(k) = \sum_{i=1}^{3} \xi_{di}(k) h_{di}(k) \end{cases} \quad (23)$$

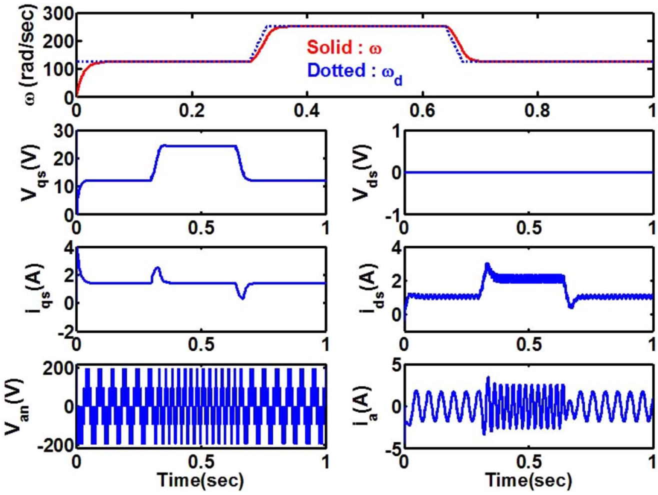

Fig. 3. Simulation results under no parameter variation.

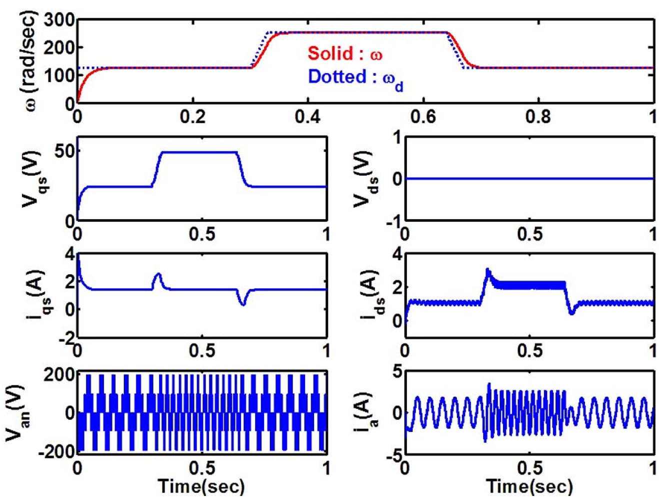

Fig. 4. Simulation results under 200% variations of some parameters (R_s, L_s, J, T_L, and λ_m).

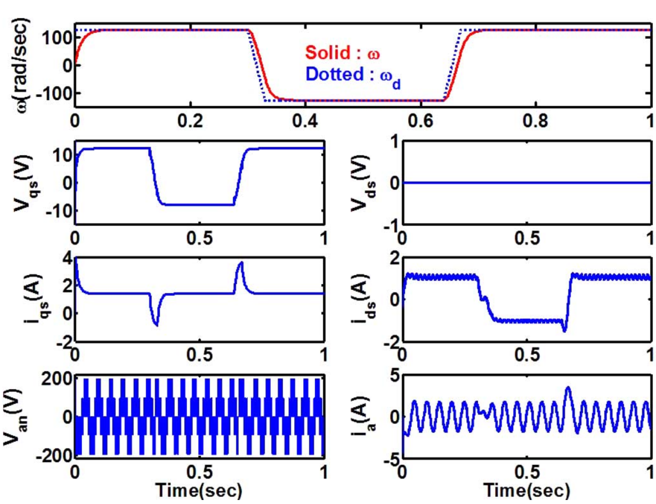

Fig. 5. Simulation results under speed reverse case.

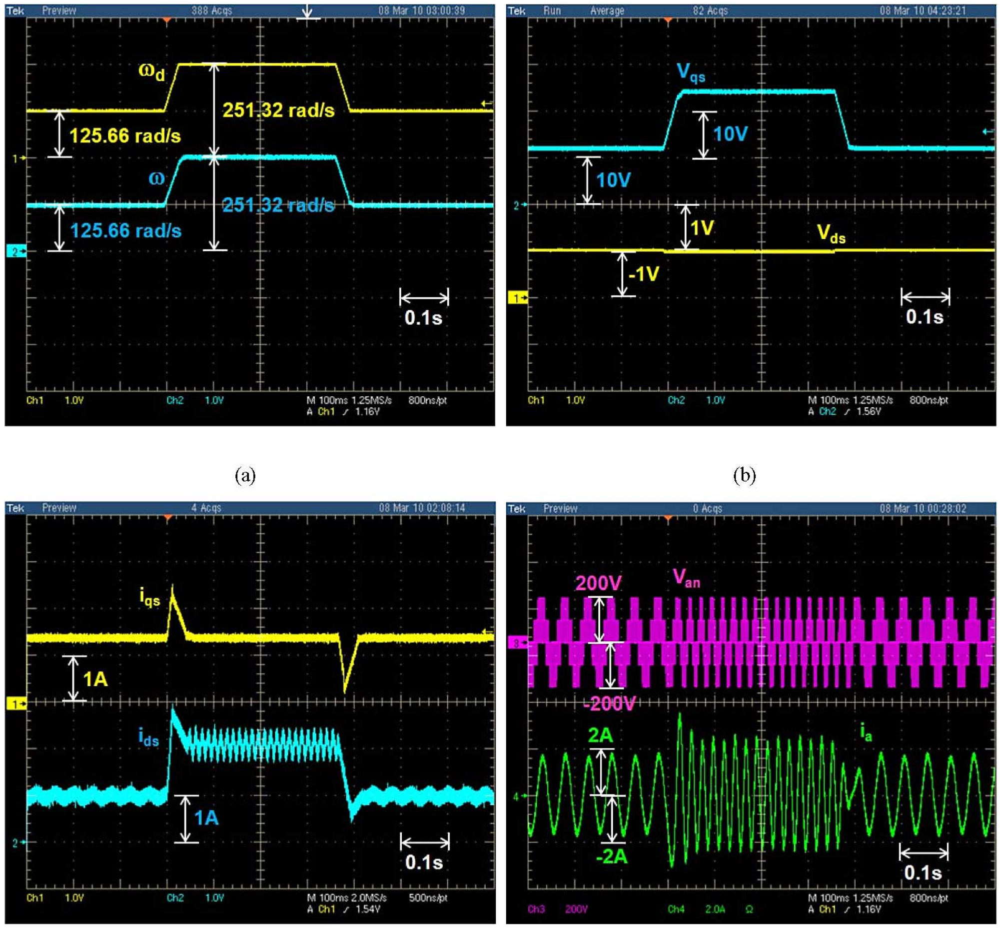

(a) (b) (c) (d)

Fig. 6. Experimental results. (a) ω_d and ω. (b) V_{qs} and V_{ds}. (c) i_{qs} and i_{ds}. (d) V_{an} and i_a.

where $\beta(k)$, $\xi_{qi}(k)$, and $\xi_{di}(k)$ are updated by the recursive equations (20)–(22). Fig. 1 shows overall block diagram of the proposed control algorithm.

V. Simulation and Experiment

For simulation and experiment, we consider a PMSM (1) with $p = 12$, $R_s = 0.99[\Omega]$, $L_s = 5.82[\text{mH}]$, $\lambda_m = 0.0791$ [V·sec/rad], $J = 0.00121[\text{kg}\cdot\text{m}^2]$, $B = 0.0003[\text{N}\cdot\text{m}\cdot\text{sec/rad}]$. With $\delta_q = 0.01$, $\delta_d = 0.001$, $\phi_{qi} = 2$, $\phi_{di} = 2$, $\gamma_q = 100$, and $\rho = 0$, we can obtain the following control law:

$$\begin{cases} V_{qs}(k) = -\omega_e(k) - \dfrac{0.01}{T}[\omega(k) - \omega(k-1)] \\ \qquad\qquad + \displaystyle\sum_{i=1}^{4} \xi_{qi}(k) h_{qi}(k) \\ V_{ds}(k) = -0.001 i_{ds}(k) + \displaystyle\sum_{i=1}^{3} \xi_{di}(k) h_{di}(k) \end{cases} \tag{24}$$

where $\xi_{qi}(k)$ and $\xi_{di}(k)$ are updated by the following recursive equations:

$$\begin{cases} \xi_{qi}(k+1) = \xi_{qi}(k) - \dfrac{1}{100} h_{qi}(k)\omega_e(k) \\ \qquad\qquad - \dfrac{1}{10000T} h_{qi}(k)[\omega(k) - \omega(k-1)] \\ \xi_{di}(k+1) = \xi_{di}(k) - \dfrac{1}{10000} h_{di}(k) i_{ds}(k) \end{cases} \tag{25}$$

and $h_q(k) = [\omega(k), i_{qs}(k), \omega(k)i_{ds}(k), 1]^T$, $h_d(k) = [i_{ds}(k), \omega(k)i_{qs}(k), 1]^T$. Fig. 2 shows the overall block diagram of the proposed PMSM control system. In simulations and experiments, the switching frequency and the sampling frequency $(1/T)$ are selected as 5[kHz], and a space vector pulsewidth modulation technique is adopted. Figs. 3 and 4 show the simulation results using Matlab/Simulink about two cases: no parameter variation and 200% variations of some parameters (R_s, L_s, J, T_L, and λ_m). In both cases, the desired motor speed (ω_d) increases from 125.66 [rad/sec] to 251.32 [rad/sec] and then decreases from 251.32 [rad/sec] to 125.66 [rad/sec]. Fig. 3 shows the simulation results (ω_d, ω, V_{qs}, V_{ds}, i_{qs}, i_{ds}, V_{an}, and i_a)

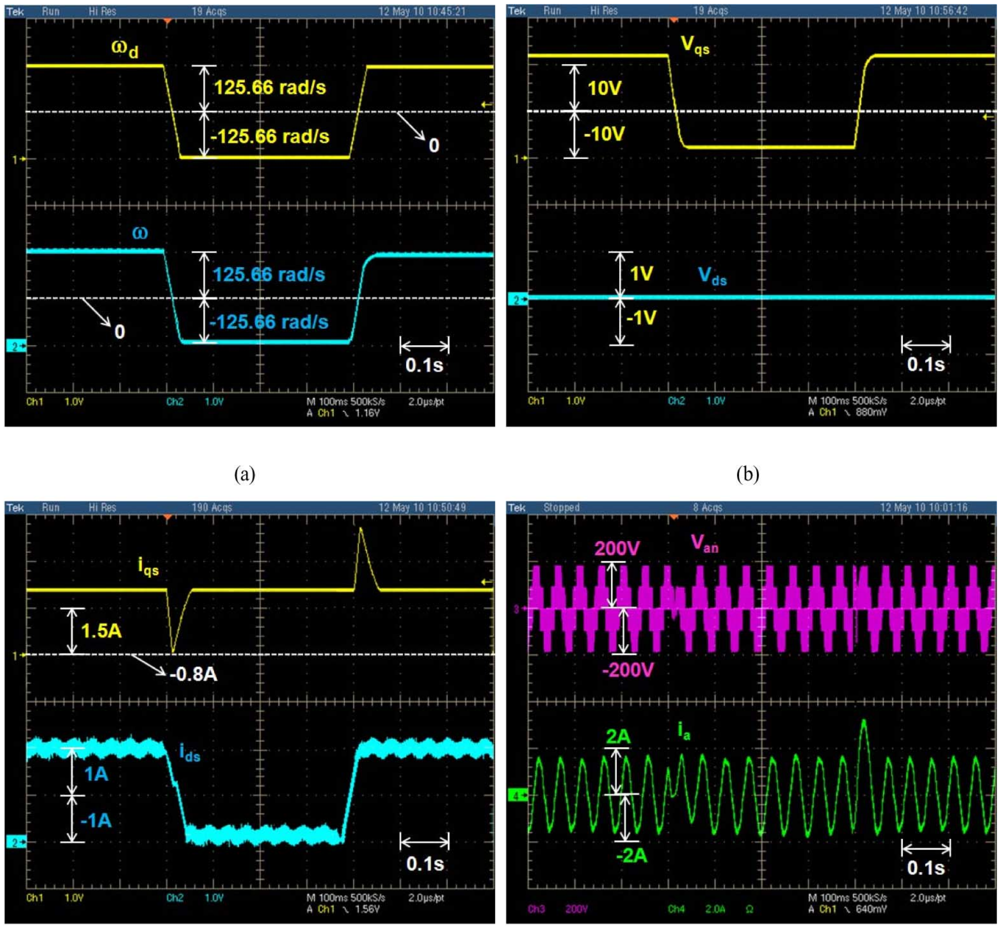

(a) (b) (c) (d)

Fig. 7. Experimental results (speed reverse case). (a) ω_d and ω. (b) V_{qs} and V_{ds}. (c) i_{qs} and i_{ds}. (d) V_{an} and i_a.

under no parameter variation. In Figs. 3 and 4, we can observe that our adaptive speed controller is very robust to model parameter and load-torque variations. Fig. 4 shows the simulation results under 200% variations of some parameters (R_s, L_s, J, T_L, and λ_m). For further verification, we also consider the case when the desired speed (ω_d) is reversed. In this case, the desired motor speed (ω_d) goes down from 125.66 [rad/sec] to –125.66 [rad/sec] and then goes up from –125.66 [rad/sec] to 125.66 [rad/sec]. Fig. 5 shows the simulation results for that case. Fig. 6 shows the experimental results about motor speed, voltage, and current under the same condition as Fig. 3. Fig. 6(a) shows the desired speed (ω_d), measured speed (ω), and Fig. 6(b) shows the q-axis and d-axis voltages (V_{qs}, V_{ds}), respectivley. Fig. 6(c) shows the measured q-axis current (i_{qs}) and d-axis current (i_{ds}), and Fig. 6(d) shows the line to neutral voltage (V_{an}) and phase a current (i_a). Fig. 7 shows the experimental results about the speed reverse case.

VI. Conclusion

We proposed an adaptive speed-regulator design method for a PMSM. The proposed adaptive speed controller is robust because it does not depend on the PMSM parameter and load-torque values. We also proved that the speed error of the closed-loop system converges to zero and the parameter adaptation error signal is bounded. Via various simulation and experimental results, it was clearly proven that the proposed adaptive speed regulator gives very remarkable speed-control performance with no information on the PMSM parameter and load-torque values.

References

[1] T.-H. Liu, H.-T. Pu, and C.-K. Lin, “Implementation of an adaptive position control system of a permanent-magnet synchronous motor and its application,” *IET Electr. Power Appl.*, vol. 4, pp. 121–130, 2010.

[2] W.-T. Su and C.-M. Liaw, “Adaptive positioning control for a LPMSM drive based on adapted inverse model and robust disturbance observer,” *IEEE Trans. Power Electron.*, vol. 21, no. 2, pp. 505–517, Mar. 2006.

[3] Y. A.-R. I. Mohamed, “A hybrid-type variable-structure instantaneous torque control with a robust adaptive torque observer for a high-performance direct-drive PMSM,” *IEEE Trans. Ind. Electron.*, vol. 54, no. 5, pp. 2491–2499, Oct. 2007.

[4] K.-H. Kim, “Model reference adaptive control-based adaptive current control scheme of a PM synchronous motor with an improved servo performance,” *IET Electr. Power Appl.*, vol. 3, pp. 8–18, 2009.

[5] C.-K. Lin, T.-H. Liu, and S.-H. Yang, “Nonlinear position controller design with input-output linearisation technique for an interior permanent magnet synchronous motor control system,” *IET Power Electron.*, vol. 1, pp. 14–26, 2008.

[6] M. N. Uddin and M. A. Rahman, “High-speed control of IPMSM drives using improved fuzzy logic algorithms,” *IEEE Trans. Ind. Electron.*, vol. 54, no. 1, pp. 190–199, Feb. 2007.

[7] Y.-S. Kung, C.-C. Huang, and M.-H. Tsai, “FPGA realization of an adaptive fuzzy controller for PMLSM drive,” *IEEE Trans. Ind. Electron.*, vol. 56, no. 8, pp. 2923–2932, Aug. 2009.

[8] K.-B. Lee and F. Blaabjerg, “Robust and stable disturbance observer of servo system for low-speed operation,” *IEEE Trans. Ind. Appl.*, vol. 43, no. 3, pp. 627–635, May/Jun. 2007.

[9] Y. Zhang, C. M. Akujuobi, W. H. Ali, C. L. Tolliver, and L.-S. Shieh, “Load disturbance resistance speed controller design for PMSM,” *IEEE Trans. Ind. Electron.*, vol. 53, no. 4, pp. 1198–1208, Aug. 2006.

[10] S. Li and Z. Liu, “Adaptive speed control for permanent-magnet synchronous motor system with variations of load inertia,” *IEEE Trans. Ind. Electron.*, vol. 56, no. 8, pp. 3050–3059, Aug. 2009.

[11] K. J. Astrom and B. Witternmark, *Computer-Controlled Systems - Theory and Design*. Englewood Cliffs, NJ: Prentice-Hall, 1990.

[12] F. L. Lewis, C. T. Abdallah, and D. M. Dawson, *Control of Robot Manipulators*. New York, NY: Macmillan, 1993.